High-Shear-Rate Behavior of Radial Hydrogenated Styrene−Isoprene and Block Ethylene−Propylene Copolymer Solutions

David C. Erickson,[†] Dongqing Li,*[,†] Tony M. White,[‡] and Jason Gao[‡]

Department of Mechanical & Industrial Engineering, University of Toronto, 5 Kings College Road, Toronto, Ontario, Canada M5S 3G8, and Imperial Oil/Products & Chemicals Division, 453 Christina Street South, P.O. Box 3022, Sarnia, Ontario, Canada N7T8C8

Using a capillary viscometry technique, the high-shear-rate behavior of two polymer additives (an ethylene−propylene block copolymer and a radial hydrogenated styrene−isoprene copolymer) in a hydrocarbon-based oil solution has been investigated. At mass concentrations of up to 2.0% for the styrene−isoprene copolymer and 1.5% for the ethylene−propylene additive, the viscosity was measured over a range of shear rates from 10^4 to 10^6 s^{-1}. To correct for the effects of viscous heating and pressure changes, a numerical correction procedure is used which reduces the experimental results to viscosity data at a common reference temperature and pressure for comparison. Over the range of shear rates examined, the styrene−isoprene solutions exhibited typical shear-thinning behavior, becoming more dramatic at higher polymer concentrations. In addition to shear thinning at the higher shear rates, a shear-thickening region was observed in the more concentrated ethylene−propylene solutions. As the polymer concentration increased, the degree of shear thickening was shown to be more severe and the critical region was observed at lower shear rates.

1. Introduction

Most base oils exhibit Newtonian behavior; i.e., the viscosity of the fluid is independent of the rate at which it is being sheared. When long-chain polymers are added as rheology modifiers to improve the high-temperature performance, the long-range interactions influence the momentum transfer normal to the flow and thus can have different influences on the viscosity of the oil depending on their concentration, type, and rate at which they are being sheared. At these high shear rates, which can be on the order of 10^6 s^{-1} in many industrial lubrication applications,[1,2] a temporary decrease in the viscosity is observed due to the alignment of these polymer molecules with the shear-rate gradient.[3] While this high-shear-rate performance is important in determining, for example, cranking resistance at startup, other applications such as pumpability of the crankcase oil have been found to be more closely related to the low-shear-rate performance.[4] Thus, an understanding of the viscosity performance of the polymer solution over a range of shear rates is critical in determining the true effectiveness of a particular additive.

Two VI (viscosity index)-improving polymer additives are of interest to this study; a radial hydrogenated styrene−isoprene copolymer and an A−B−A block-type ethylene−propylene copolymer (both supplied by Imperial Oil). The rheology of block styrene−isoprene copolymers has been investigated in various forms by a number of authors;[5−7] however, a literature review shows little work has been done on the radial form. The ethylene−propylene copolymer used here is comprised of approximately 60% ethylene units concentrated in the middle of the chain (the polymer is manufactured in a tubular reactor, which allows the position of the ethylene units along the chain to be controlled). At low temperatures the ethylene segments tend to associate, reducing the overall hydrodynamic volume of the polymer and thus the low-temperature viscosity of the solution, giving it a cold cranking viscosity advantage over more amorphous polymers. The rheology of similar ethylene−propylene block copolymers has been studied by a number of investigators.[8−10] For example, Han and Rao[10] measured the high-shear-rate behavior of such a polymer at 240 °C, while Kucks et al.[9] studied its aggregation in different hydrocarbon solvents. Note that all of these studies have concentrated on either high-temperature or low-shear-rate measurements.

The purpose of this study is to investigate the high-shear-rate behavior of these two different polymer additives in a hydrocarbon base oil (EHC-45; Imperial Oil Product). At mass concentrations ranging from 0 to 2.0% for the styrene−isoprene additive and from 0 to 1.5% for the ethylene−propylene polymer, the viscosity has been measured at wall shear rates ranging from 10^4 to 10^6 s^{-1}, using a capillary viscometer. A data analysis procedure is presented which uses a numerical model of capillary flow to account for changes in the viscosity along the length of the capillary due to temperature (viscous heating) and pressure effects. As part of the correction procedure, additional experiments were conducted to determine the viscosity dependence on temperature for the solutions of interest.

2. Experimental Section

2.1. Polymer Characterization and Solution Preparation. The molecular weight distribution of the

* Corresponding author. E-mail: dli@mie.utoronto.ca. Fax: (416) 978-7753.
[†] University of Toronto.
[‡] Imperial Oil/Products & Chemicals Division.

10.1021/ie0100941 CCC: $20.00
Published on Web 07/06/2001

two polymers was determined using a gel permeation chromatography technique which yielded $M_w = 497\,000$ and $M_n = 472\,000$ for the styrene−isoprene copolymer and $M_w = 235\,000$ and $M_n = 205\,000$ for the ethylene−propylene copolymer. The analyses were carried out in Prof. Manners' laboratory in the Department of Chemistry, University of Toronto, by using a Waters 2690 separation unit and a Viscotek T90A dual light scattering and viscometry detector.

Using the criteria $c^*[\eta] = 1$ and the intrinsic viscosities of similar polymer solutions from Filiatrault and Delmas,[11] a critical concentration of approximately 0.5% was estimated for the ethylene−propylene polymer, which is of the order quoted in Kucks et al.[9] Therefore, the higher concentrations of this polymer examined in this study are likely to enter the semidilute range, where significant coil overlap begins. The intrinsic viscosity of the styrene−isoprene copolymer in similar solutions was not known; however, the order of magnitude estimates from ref 12 suggest that the solutions examined here lie within the dilute range.

Solution preparation was done by dissolving the polymers in the base oil by heating the solution to over 100 °C and intermittently stirring over the course of 48 h. At this temperature evaporative losses of the base oil were found to be very small, less than 0.1%, and did not affect the final solution concentration. All solution preparation was carried out in a fume hood.

2.2. Capillary Viscometer. Generally, capillary viscometers can be divided into two classifications: constant flow rate and constant pressure. Because the shear rate is uniquely determined by the geometric properties of the capillary and the volumetric flow rate, constant-flow-rate designs have the advantage of being able to repeat tests for different solutions at nearly the same shear rate. As such, this type was selected and built for this study using a Ruska Instruments high-pressure precision piston pump, which had a flow range of between 2.5 and 560 mL/h to an accuracy of ±0.02 mL/h at pressures as high as 70 MPa. The use of a piston type is preferred over a gear-type positive displacement pump, which may preshear the fluid prior to reaching the capillary, resulting in an immeasurable amount of permanent viscosity loss.[13]

The capillary tubes used to make the shear viscosity measurements were all 115 μm in diameter and varied from 10.8 to 12.9 mm in length, while the temperature viscosity measurements were made using a 235 μm diameter capillary of 51.2 mm length. In general, shorter capillaries are preferred to longer ones to reduce the required pressure drop at a given flow rate. The low Reynolds number regime observed in this study, $Re <$ 45, allowed for such short tubes to be used while keeping the entrance length to less than 2% of the total length. The total pressure drop across the capillary was measured using a Validyne differential pressure transducer, calibrated by a dead-weight tester, with a 0.5% full-scale accuracy.

2.3. Experimental Procedure. The high-shear-rate tests were conducted at nine different wall shear rates ranging from 10^4 to 10^6 s^{-1}. At each shear rate the flow-rate measurement was made through mass collection, and the capillary wall temperature was recorded using a type k thermocouple. Temperature−viscosity measurements, for use in the correction procedure, were conducted by preheating the test solution to the desired temperature in a heating coil submersed in a water bath. All temperature−viscosity measurements were made at the same low wall shear rate, 1.2×10^4 s^{-1}, to ensure that both non-Newtonian influences and internal heat generation were minimized.

3. Data Analysis

While it is relatively easy to design and build a capillary viscometer where measurements of the pressure drop and volume flow rate can be made with high accuracy, secondary flow effects can make it difficult to extract meaningful results. Ideally, one would like to account for these effects in such a way that the experimental data can be reduced to viscosity data at a common temperature and pressure for comparison. Previous studies have accomplished this by either experimental calibration[4,14] or a mathematical solution to the Navier−Stokes equations.[15−19] The former generally requires that extensive experimental measurements be made for several different Newtonian fluids over a range of conditions, and the results are compared with previously known viscosity values to produce a series of calibration curves.[14] Mathematical techniques, however, do not require such extensive background data and can be applied directly to experimental results.

In all cases the mathematical treatment involves a simultaneous solution of the equations for continuity, momentum, and energy. Some analytical solutions have been proposed, for example, that by Kearsley;[15] however, the assumptions required to reduce the equations to a solvable form limit their widespread applicability. More popular in modern studies are numerical solutions to a more exact form of the equations. Gerrard et al.[16,17] developed a two-dimensional solution using a finite difference scheme, which considered both temperature and pressure effects on the viscosity of a Newtonian fluid, for the cases of an adiabatic and isothermal capillary wall. Their results showed that significant temperature gradients exist within the channel, resulting in large changes in the fluid viscosity along the length of the channel. Duda et al.[19] further extended the model to cases of higher Reynolds number and used it to predict the shear behavior of non-Newtonian fluid solutions.

When common scaling arguments related to the large L/D ratio of the capillary are applied,[16,17] the governing equations (in dimensional form) reduce to eqs 1a (continuity), 1b (momentum), and 1c (energy), where v_r

$$\frac{1}{r}\frac{\partial}{\partial r}(rv_r) + \frac{\partial v_z}{\partial z} = 0 \tag{1a}$$

$$\frac{\partial P}{\partial z} - \frac{1}{r}\frac{\partial}{\partial r}(\tau_{rz}) = 0 \tag{1b}$$

$$\rho c_p\left(v_z\frac{\partial T}{\partial z} + v_r\frac{\partial T}{\partial r}\right) - k\left(\frac{\partial^2 T}{\partial r^2} + \frac{1}{r}\frac{\partial T}{\partial r}\right) = \tau_{rz}\left(\frac{\partial v_z}{\partial r}\right) \tag{1c}$$

and v_z are the components of velocity in the radial and axial directions, τ_{rz} is the shear stress, ρ is the density, k is the thermal conductivity, and c_p is the specific heat. In addition to the dimensional scaling assumptions, this form of the equations assumes that the Reynolds number is sufficiently low such that the fluid remains laminar and the entrance region is small and assumes that density, thermal conductivity, and specific heat are all constant. With the elimination of the momentum

convection terms in eq 1b, it has been assumed that the flow is sufficiently unidirectional such that momentum diffusion dominates. Though this assumption is likely valid for this geometry, it is important still to note that in-channel viscosity gradients will result in a small radial velocity component, which has been incorporated into eq 1c for completeness.

Under the same dimensional scaling arguments, the shear stress distribution can be described by $\tau_{rz} = \mu\, \partial v_z/\partial r$, where, in general, μ is a function of temperature, pressure, and shear rate for non-Newtonian fluids such as those considered here. In most previous studies,[15−18] it has been assumed that, for the purposes of predicting the magnitude of viscous heating, a solution based on a theoretical Newtonian fluid can be made. Duda et al.[19] discussed this assumption and showed that it is generally valid and, however, tends to yield slightly higher viscosity results at very high shear rates. To compensate for this, they suggested an iterative procedure for determining the power law index, given that the low-shear-rate viscosity and the range of the initial Newtonian plateau are known; however, they acknowledge that this technique is largely empirical because the index is adjusted to obtain agreement between theory and experiment. While this technique may be applicable to a single fitted parameter, more complex fluids, where multiple fitted parameters would be required, implementation of such an iterative step may not be successful and could lead to even larger errors. Therefore, in this study the theoretical Newtonian fluid assumption is used for determining the magnitude of the shear heating, realizing that while the majority of the effect will be captured, the procedure may lead to a slight overcorrection at higher shear rates.

In most studies it is assumed that the viscosity depends in some fashion exponentially on both pressure and temperature; see, for example, refs 13, 16, 17, 20, and 21. When the two influences are superimposed, the simplest viscosity transport relation is given by eq 2,

$$\mu(T,P) = \mu_0 e^{k_p P - \alpha \Delta T} \tag{2}$$

where ΔT is the temperature rise above T_0, α is the temperature viscosity coefficient, k_p is the pressure coefficient of viscosity, P is the gauge pressure, and μ_0 is the viscosity at atmospheric pressure and temperature. Note that in this expression the effects of temperature and pressure have been considered to be additive, which is a common assumption made by a number of authors; again see ref 20.

By incorporating the measured volume flow rate into the analysis through the global continuity equation, eq 3,

$$Q = 2\pi \int_0^R v_z r\, dr \tag{3}$$

and subjecting eq 1 to the appropriate boundary conditions (see section 4.2 for a discussion), the above equations can be solved for the unknowns $v_z(r,z)$, $v_r(r,z)$, $P(z)$, and $T(r,z)$ and the desired apparent viscosity in the absence of temperature and pressure effects, μ_0. In general, the same iterative scheme as that used by Gerrard et al.[16,17] has been employed to solve the equations. When applied to non-Newtonian fluids, the apparent viscosity and apparent shear rate, γ_{aw}, obtained from this analysis were then corrected using the Weissenberg−Rabinowitsch[22] equation as

$$\dot{\gamma}_w = \frac{1}{4}\dot{\gamma}_{aw}\left[3 + \frac{d(\ln Q)}{d(\ln \Delta P)}\right] \tag{4a}$$

$$\mu_w = 4\mu_0\left[3 + \frac{d(\ln Q)}{d(\ln \Delta P)}\right]^{-1} \tag{4b}$$

where γ_w and μ_w are the true shear rate and viscosity at the capillary wall.

In addition to the above, a kinetic energy correction is required as a result of the fact that the entrance pressure was measured in the fluid static state while the exit pressure is only known for the dynamic case. As a result, the dynamic pressure head of the fluid exiting the capillary must be subtracted from the measured pressure drop as

$$\Delta P = P_{obs} - \rho\left(\frac{Q}{A}\right)^2 \tag{5}$$

where Q/A is the volume flow rate divided by the cross-sectional area of the capillary, equivalent to the average velocity of the exiting stream, and P_{obs} is the observed static pressure at the entrance to the channel. While in studies conducted for lower viscosity fluids, this correction has been shown to be significant;[13] the higher pressures observed in this study limit the effect of this correction to less than 2% of P_{obs}.

Table 1. Best-Fit Values of Viscosity Temperature Coefficient, α, for Styrene−Isoprene (SI) and Ethylene−Propylene (EP) Copolymer Solutions

solution	α	R^2	solution	α	R^2
base oil	0.053	0.99	0.5% EP	0.56	0.99
0.5% SI	0.053	0.99	1.0% EP	0.55	0.98
1.0% SI	0.053	0.99	1.5% EP	0.51	0.98
1.5% SI	0.053	0.99			
2.0% SI	0.051	0.99			

4. Evaluation of the Analysis Procedure

The capillary flow model will be validated using the EHC 45 base oil, which is known to exhibit Newtonian behavior. The fluid had a density of 850 kg/m^3, a specific heat of 1.9×10^3 J·K/Kg, a thermal conductivity of 142×10^{-3} W·K/m, and a pressure viscosity coefficient of 0.25×10^{-8} 1/Pa, which is of the same order as that quoted for paraffinic base stocks in ref 13.

4.1. Temperature Viscosity Coefficient. As part of the data correction procedure, the temperature viscosity coefficient, α, was determined experimentally using the technique described in section 2.3. The tests were conducted over a 20 °C range above the ambient temperature, which was the limit of the expected viscous heating. As is mentioned above, all tests were conducted at a constant shear rate near the lower end of those examined here (1.2×10^4 s^{-1}) in order to ensure that internal heat generation was negligible and that any shear-related non-Newtonian influences did not affect the result.

The data from these experiments were fitted to an exponential curve using a least-squares regression algorithm to determine the best-fit value of the coefficient α in eq 2, the results of which are listed in Table 1. On the basis of these results, it is apparent that the value of the viscosity temperature coefficient, α, does not change appreciably because of the addition of the

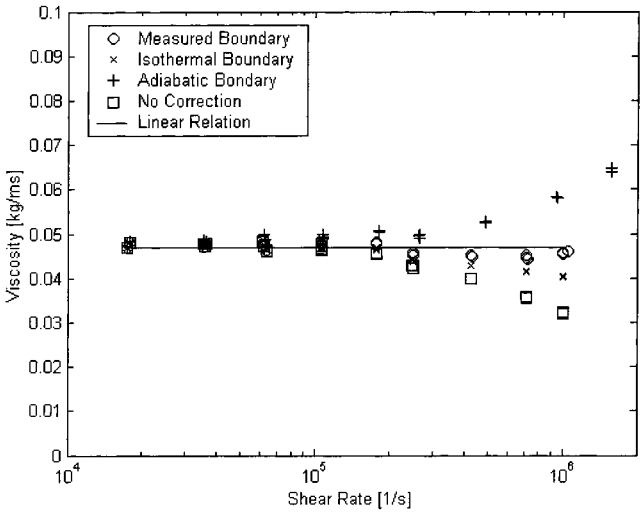

Figure 1. Effectiveness of the capillary flow model at correcting for the effects of pressure and temperature dependence on viscosity using various capillary wall temperature boundary conditions.

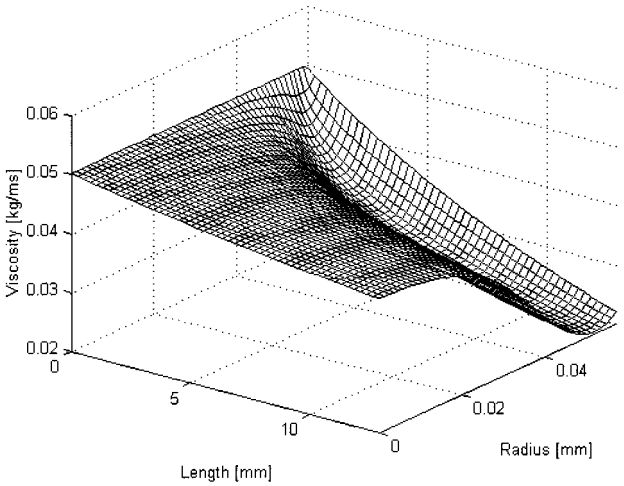

Figure 2. Viscosity profile of the Newtonian base oil flowing through a capillary at a wall shear rate of 10^6 s^{-1}.

polymer over the range of temperatures of interest here, staying within ±4% of its median value of $\alpha = 0.053$ 1/K. The high R^2 values suggest that indeed the assumption of an exponential viscosity temperature relationship is indeed valid for all of the examined polymer concentrations.

4.2. Analysis of Capillary Flow Model and Boundary Conditions. In section 3, the capillary flow model was developed, with the purpose of predicting and correcting for viscosity gradients due to changes in pressure and temperature along the capillary axis; however, the accuracy of such a model is largely dependent on the proper assignment of the boundary conditions. While velocity boundary conditions are relatively straightforward ($v_z = 0$ and $v_r = 0$ at the capillary wall and $v_r = 0$ $\partial v_z/\partial r = 0$ about the symmetry axis), the temperature conditions are less so. As is commonly done,[16,17,19] this study assumes a uniform entrance profile ($T = T_0$) and temperature symmetry about the capillary axis ($\partial T/\partial r = 0$). Both Gerrard et al.[16,17] and Duda et al.[19] have compared the results of using isothermal and adiabatic boundary conditions at the capillary wall to experimental results and concluded that generally the isothermal condition is more accurate; however, it is generally accepted that the true boundary condition would lie somewhere between these two extremes. In this study the effectiveness of the isothermal and adiabatic boundary conditions used in previous studies will be compared with a prescribed boundary temperature corresponding to that measured during the experiment.

Figure 1 compares the results of the three boundary conditions of interest with the uncorrected viscosity results for the EHC 45 base oil (note that all results are shown and no data averaging was used). As can be seen, the raw, uncorrected data mistakenly predicts a decreasing trend in viscosity as the wall shear rate increases. When the numerical procedure is used to correct these results, Figure 1 shows that the different capillary wall temperature boundary conditions yield dramatically different results. As is apparent the prescribed temperature boundary condition yields a nearly perfect Newtonian result, while the isothermal condition does not provide sufficient correction and the adiabatic condition overcorrects. On the basis of these results, the prescribed temperature boundary condition was used in the final analysis to correct for pressure and temperature effects on viscosity.

Figure 2 shows the viscosity profile in the capillary for the base oil at a wall shear rate of 10^6 s^{-1} as predicted using the capillary flow model with the prescribed temperature boundary condition. As can be seen, significant viscosity gradients exist within the capillary, with the overall value ranging from over 0.05 kg/m·s at the entrance to just above 0.02 kg/m·s at the minimum near the channel wall at the exit. Because of the high shear rate and thus high degree of viscous heating in this region, the most significant viscosity deviations are observed nearest the channel wall. Nearer the center of the channel, heat generation is much less significant; however, a lower viscosity is still predicted because of the pressure drop along the capillary axis and the small amount of radial heat condition from the regions nearest the wall.

5. Results and Discussion

As mentioned earlier the main purpose of this study was to investigate the high-shear-rate viscosity of the radial hydrogenated styrene−isoprene and the ethylene−propylene viscosity improving polymer additives in the EHC 45 base oil. Parts a and b of Figure 3 show the relationship between the viscosity at room temperature and pressure and the wall shear rate for the two polymer additives. Because only relatively small amounts of the additives were used in each case, the thermal properties listed above for the base oil were assumed to be constant, independent of the polymer concentration for use in the data analysis procedure. All results are shown, and no data averaging was used.

In the case of the styrene−isoprene additive (Figure 3a), it is apparent that for all concentrations the viscosity drops nearly linearly with logarithmic shear rate, over the examined range of shear rates. This effect is very pronounced at the higher concentration solutions and decreases gradually until nearly Newtonian behavior was observed at the lower concentration solutions. This shear-thinning behavior is typical of such oil-based polymer solutions and results from the shear gradient aligning the polymer molecules in the flow direction. As the rate of shear increases, this alignment becomes stronger until a point is reached where little or no more alignment can occur, at which point increasing the shear

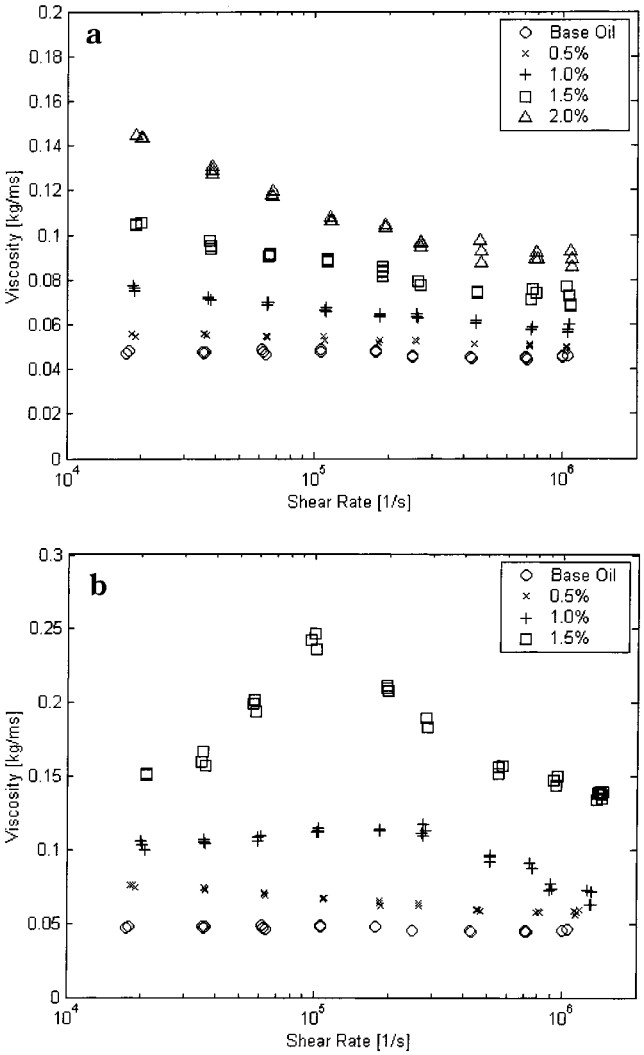

Figure 3. Relationship between the viscosity and shear rate of (a) a radial hydrogenated styrene−isoprene copolymer and (b) an A−B−A block-type ethylene−propylene copolymer solutions at various mass concentrations.

rate further has no significant effect on the viscosity. Because all polymer concentrations show a continuously decreasing viscosity up to and including the highest attainable shear rate, it can be assumed that this point of transition to Newtonian behavior lies somewhere beyond the 10^6 s^{-1} shear rate.

As can be seen in Figure 3b, the ethylene−propylene polymer solutions exhibited a much more complicated and atypical viscosity behavior. While shear thinning was observed at the highest shear rates for all concentrations, the two most highly concentrated solutions appear to exhibit a shear-thickening stage, where the viscosity was observed to increase to as much as 150% of its prethickening value before shear thinning was again exhibited. The range over which the apparent shear thickening was observed varied from 3×10^4 to 3×10^5 s^{-1}, depending on the concentration, with the critical region appearing at a lower shear rate for higher concentrations.

Before examination of the possible shear-thickening mechanism present here, a more thorough discussion of the different phenomena associated with the measurement technique, such as slip flow, surface adsorption, and viscoelastic influences, which may contribute to such behavior is warranted. Slip flow is a well-observed phenomenon in polymer rheology, the analysis of which dates back to Mooney's original derivations.[23] Since that time, authors have explained the apparent slip originally in terms a depleted layer near the capillary wall[24] or more recently through cross-streamline polymer migration.[25,26] In either case the presence of a slip layer would result in a decrease in the apparent viscosity and thus could not account for the anomalous behavior observed here. Others, for example, Cohen,[27] have examined the role of surface adsorption on the flow of polymer solutions through capillaries. Their studies revealed that in all cases the thickness of the adsorbed layer decreased with increasing shear stress and thus could not account for this behavior.

When forced into the capillary, work is done on a viscoelastic fluid to set up elastic stresses as it converges through the narrow opening. This work is recovered after the fluid leaves the capillary; however, the pressure work done to induce the stresses is lost. Moan et al.[28] have examined this effect and have shown that above a certain critical shear rate this increased pressure drop becomes significant and could yield results suggesting an apparent increase in viscosity. This effect was shown to be strongly dependent on the Reynolds number and the L/R ratio of the capillary. To test for this here, the high-concentration experiments were repeated with a different capillary and a much smaller L/R (89 compared with 224) where this influence should be significantly more dramatic. Both capillaries exhibited the exact same behavior, suggesting that this effect is not the dominant cause of the viscosity increase.

In their theoretical and experimental works, Peterlin and co-workers[29,30] investigated the effects of intramolecular hydrodynamic interactions on the intrinsic viscosity of polymer solutions. By using a hydrodynamic resistance coefficient to account for the nonuniform changes in the intermolecular distances, they showed that the intrinsic viscosity should initially decrease to a minimum and then increase in what they called the upturn effect. The behavior was then observed experimentally in a highly viscous solvent ($\mu = 0.5$ kg/m·s) with a very high molecular weight polymer ($M_w = 7 \times 10^6$). Though this effect cannot be completely disregarded, the high solvent viscosity and polymer molecular weights that are generally required suggest that this effect is again not dominant here.

The experimental evidence available to date is insufficient to provide detailed information regarding the shear-thickening mechanism present here; however, a brief examination of some of the possible causes is warranted. A number of authors[31−36] have investigated the role of flow-induced phase separations and concentration fluctuations on the rheological properties of polymer solutions. Studies such as Yanase et al.[33] and Moldenaers et al.[32] have observed drastic shear thickening and have attributed it to a transition in the direction of the alignment of concentration fluctuations from the vorticity axis to the flow axis. McHugh and co-workers have examined the influences of phase transformations leading to flow-induced crystallization[37,38] and the results of this behavior on the rheological properties of several crystallizable polymer solutions.[39] Their results were very similar to the behavior shown in Figure 3b.

Ballard et al.[40] as well as others[41] have proposed detailed molecular models describing the role of intermolecular associations to the formation of shear-induced gel-type network structures (such a formation differs

from a true gel in that it does have a finite viscosity due to the transient nature of the cross-links). As is detailed in their paper,[40] intramolecular associations present in the quiescent medium are broken at low shear rates as the polymer molecule is extended and begins to align itself with the shear gradient. Above a critical shear rate, when a sufficient number of the intramolecular associations have been broken, it is thought that the molecules will become entangled and the associations will reform in an intermolecular fashion because the molecule is now in an elongated state, resulting in an increase in the solution viscosity. As the shear rate is further increased, the shear gradient is sufficiently strong to disentangle the molecules and break the intermolecular associations leading to a final shear-thinning region. As mentioned earlier this ethylene−propylene polymer is known to exhibit intermolecular associations at the temperatures examined here, and the concentrations where the shear-thickening behavior was observed are above the critical concentration where significant coil overlap exists, thereby making such intermolecular associations plausible. However, with the limited data available here, it is impossible to provide an exact interpretation of the shear-thickening mechanism.

To emphasize the concentration dependence on viscosity, the two polymer solutions are compared at a relatively low shear rate of 2×10^4 s^{-1} (Figure 4a) and a high shear rate of 10^6 s^{-1} (Figure 4b). The results presented in these figures represent the average result of measurements taken at equivalent shear rates. As a result of the shear thinning, it is apparent that at the lower shear rate (Figure 4a) the 2% styrene−isoprene solution shows a viscosity increase of nearly 300% over the base oil, while at the higher shear rate (Figure 4b), the improvement is reduced to 200% of the base oil viscosity. In all cases, the ethylene−propylene polymer exhibited a higher viscosity at a given concentration (than the styrene−isoprene polymer), especially at the higher shear rates where the results are influenced by the shear-thickening stage.

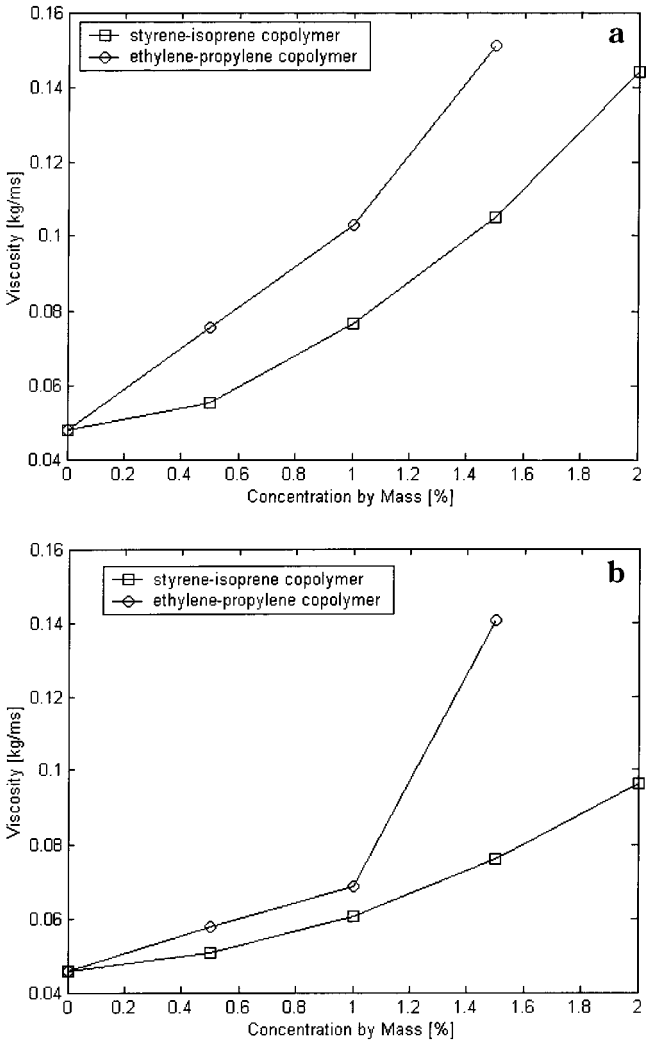

Figure 4. Viscosity increase with polymer concentration at (a) low shear rates, 2×10^4 s^{-1}, and (b) high shear rates, 10^6 s^{-1}.

6. Conclusions

The purpose of this study was to investigate the non-Newtonian behavior of two different polymer additives, a radial hydrogenated styrene−isoprene copolymer and an A−B−A type block ethylene−propylene copolymer, in an EHC 45 base oil. Tests were conducted using a capillary viscometer to characterize the viscosity behavior of the polymer solutions over a range of shear rates from 10^4 to 10^6 s^{-1}. A numerical data reduction procedure was developed which used further experimental results, detailing the temperature−viscosity behavior of the solutions, to account for the effects of pressure and viscous heating and reduce the data to a common reference pressure and temperature for comparison.

The capillary flow model showed that indeed significant viscosity gradients exist within the capillary, and failure to account for these can lead to significant errors. In general, the model was shown to be most successful when a prescribed temperature boundary condition, consistent with that measured experimentally, was applied at the channel wall. Adiabatic and isothermal boundary conditions were less successful and either overcorrected (adiabatic) or undercorrected (isothermal) the experimental results.

The radial hydrogenated styrene−isoprene copolymer additive exhibited typical shear-thinning behavior over the range of shear rates examined. Generally, the effect was more dramatic in the higher concentration solutions; however, in all cases a linear viscosity decrease with logarithmic shear rate was observed. The ethylene−propylene polymer additive exhibited more atypical viscosity behavior in that a region of shear thickening was observed in the more highly concentrated solutions. As the polymer concentration was increased, the degree of shear thickening increased and the critical region over which it occurs was observed at lower shear rates.

Acknowledgment

The authors thank Professor Ian Manners and Kevin Kulbaba in the Department of Chemistry, University of Toronto, for performing the GPC analysis of the polymers used in this study. The authors also acknowledge the financial support of the Natural Sciences and Engineering Research Fund and Imperial Oil through scholarships to D.C.E. and through a research grant to D.L.

Literature Cited

(1) McMillan, M. L.; Murphy, C. K. Temporary viscosity loss and its relationship to journal bearing performance, SAE 780374. *The relationship between engine oil viscosity and engine performance—part III*; SAE SP-429 (ASTM STP-621-52), 1978.

(2) Bartz, W. J.; Wiemann, W. Determination of the cold flow behavior of multigrade engine oils, SAE 770630. *The relationship between engine oil viscosity and engine performance—part II*; SAE SP-419 (ASTM STP 621−51), 1977.

(3) Metznew, A. B. Non-Newtonian technology: fluid mechanics, mixing and heat transfer. *Adv. Chem. Eng.* **1956**, *77*, 1.

(4) Rein, S. W.; Alexander, D. L. Development of a high shear rate capillary viscometer for engine oils, SAE 800363. *The relationship between engine oil viscosity and engine performance—parts V and VI*; SAE SP-460 (ASTM STP-621-S4), 1980.

(5) Watanabe, H.; Sato, T.; Osaki, K.; Yao, M.-L.; Yamagishi, A. Rheological and dielectric behavior of a styrene−isoprene−styrene triblock copolymer in selective solvents. 2. contribution of loop-type middle blocks to elasticity and plasticity. *Macromolecules* **1997**, *30*, 5877.

(6) Roy, D.; Gupta, B. R. Rheological behavior of short carbon fibre filled thermoplastic elastomer based on styrene−isoprene−styrene block copolymer. *J. Appl. Polym. Sci.* **1993**, *49*, 1475.

(7) Bahadur, P.; Sastry, N. V.; Marti, S.; Riess, G. Micellar behavior of styrene−isoprene block copolymers in selective solvents. *Colloids Surf.* **1985**, *16*, 337.

(8) Li, S.; Järvelä, P. K.; Järvelä, P. A. A comparison between apparent viscosity and dynamic complex viscosity for polypropylene/maleated polypropylene blends. *Polym. Eng. Sci.* **1997**, *37* (1), 18.

(9) Kucks, M. J.; Ou-Yang, H. D.; Rubin, I. D. Ethylene−propylene aggregation in selective hydrocarbon solvents. *Macromolecules* **1993**, *26*, 3846.

(10) Han, H. D.; Rao, D. A. Measurement of the rheological properties of thermoplastic elastomers. *J. Appl. Polym. Sci.* **1979**, *24*, 225.

(11) Filiatrault, D.; Delmas, G. Intrinsic Viscosities and Huggins' Constant for Ethylene−Propylene Copolymers. 1. Effect of the Correlations of Orientations in the Pure Components or in the Solutions on the Solvent Quality. Viscosities in linear Alkanes and Three Highly Branched Alkanes. *Macromolecules* **1979**, *12* (1), 65.

(12) Freemen, W. J. Characterization of polymers. In *Encyclopedia of Polymer Science and Engineering*; Mark, H. F., Bikales, N. M., Overberger, C. W., Menges, G., Eds.; John Wiley and Sons: New York, 1985.

(13) Hewson, W. D.; Carey, L. R. High shear rate viscosity of engine oils. *Fuels & Lubricants*; SAE: Baltimore, MD, 1980; SAE 801394.

(14) Graham, E. E.; Klaus, E. E.; Badgley, R. S. Determination of the viscosity-shear behavior of polymer containing fluids using a single pass, high-shear capillary viscometer. SAE 841391, 1984.

(15) Kearsley, E. A. The viscous heating correction for viscometer flows. *Trans. Soc. Rheol.* **1962**, *VI*, 253.

(16) Gerrard, J. E.; Steidler, F. E.; Appeldoorn, J. K. Viscous heating in capillaries: the adiabatic case. *Ind. Eng. Chem. Fundam.* **1965**, *4*, 332.

(17) Gerrard, J. E.; Steidler, F. E.; Appeldoorn, J. K. Viscous heating in capillaries: the isothermal wall case. *Ind. Eng. Chem. Fundam.* **1966**, *5*, 260.

(18) Davies, C. E.; Pemberton, S. T.; Abrahamson, J. Capillary viscometry of a New Zealand coal at high pressures and shear stresses. *Fuel* **1983**, *62*, 417.

(19) Duda, J. L.; Klaus, E. E.; Lin, S. C. Capillary viscometry study of non-Newtonian fluids: influence of viscous heating. *Ind. Eng. Chem. Res.* **1988**, *27*, 352.

(20) Carreau, P.; De Kee, D.; Chhabra, R. *Rheology of Polymeric Systems*; Hanser Gardner: New York, 1997.

(21) Warren, R. C. Viscous Heating. In *Rheological Measurement*; Collyer, A. A., Clegg, D. W., Eds.; Chapman & Hall: London, 1998.

(22) Macosko, C. *Rheology Principals, Measurement and Applications*; VCH: New York, 1994.

(23) Money, M. Explicit Formulas for Slip and Fluidity. *J. Rheol.* **1931**, *2*, 210.

(24) Chauveteau, G. Rodlike Polymer Solution Flow through Fine Pores: Influence of Pore Size on Rheological Behavior. *J. Rheol.* **1982**, *26*, 111.

(25) Cohen, Y.; Metzner, A. B. An analysis of apparent slip flow of polymer solutions. *Rheol. Acta* **1986**, *25*, 28.

(26) Ianniruberto, G.; Greco, F.; Marricci, G. The Two-Fluid Theory of Polymer Migration in Slit Flow. *Ind. Eng. Chem. Res.* **1994**, *33*, 2404.

(27) Cohen, Y. Hydrodynamic Thickness of Adsorbed Polymers in Steady Shear Flow. *Macromolecules* **1988**, *21*, 494.

(28) Moan, M.; Chauveteau, G.; Ghoniem, S. Entrance effect in capillary flow of dilute and semidilute polymer solutions. *J. Non-Newtonian Fluid Mech.* **1979**, *5*, 463.

(29) Peterlin, A. Gradient dependence of intrinsic viscosity of freely flexible linear macromolecules. *J. Chem. Phys.* **1960**, *33*, 1799.

(30) Bianchi, U.; Peterlin, A. Upturn effect in the non-Newtonian intrinsic viscosity of polymer solutions. II. Polyisobutylene in Polybutene Oil. *J. Polym. Sci. A-2* **1968**, *6*, 1011.

(31) Saito, S.; Matsuzaka, K.; Hashimoto, T. Structures of a Semidilute Polymer Solution under Oscillatory Shear Flow. *Macromolecules* **1999**, *32*, 4879.

(32) Moldanaers, P.; Yanase, H.; Mewis, J.; Fuller, G. G.; Lee, C.-S.; Magda, J. J. Flow-Induced Concentration fluctuations in polymer solutions: Structure/property relationships. *Rheol. Acta* **1993**, *32*, 1.

(33) Yanase, H.; Moldenaers, P.; Mewis, J.; Abertz, V.; van Egmond, J.; Fuller, G. G. Structure and dynamics of a polymer solution subject to flow-induced phase separation. *Rheol. Acta* **1991**, *30*, 89.

(34) Onuki, A. Elastic Effects in the Phase Transition of Polymer Solutions under Shear Flow. *Phys. Rev. Lett.* **1989**, *62*, 2472.

(35) Barsukov, I. A.; Yemel'yanov, D. N.; Kamskii, R. A.; Bobykina, N. S. Aspects of the Rheological Behavior of Polymer Solutions in Conditions of Phase Separation. *Polym. Sci. U.S.S.R.* **1989**, *31*, 1534.

(36) Ver Strate, G.; Philippoff, W. Phase Separation in Flowing Polymer Solutions. *J. Polym. Sci. B* **1974**, *12*, 267.

(37) Rietvel, J.; McHugh, A. J. Flow induced fibrillar formation process in poiseuille flow. *J. Polym. Sci., Polym. Lett. Ed.* **1983**, *21*, 919.

(38) McHugh, A. J.; Blunk, R. H. Studies of fiber formation in tubular flow for polypropylene and poly(ethylene oxide). *Macromolecules* **1986**, *19*, 1249.

(39) Vrahopoulou, E. P.; McHugh, A. J. Shear-thickening and structure formation in polymer solutions. *J. Non-Newtonian Fluid Mech.* **1987**, *25*, 157.

(40) Ballard, M. J.; Buscall, R.; Waite, F. A. The theory of shear-thickening polymer solutions. *Polymer* **1988**, *29*, 1287.

(41) Witten, T. A.; Cohen, M. H. Cross-Linking in shear thickening ionomers. *Macromolecules* **1985**, *18*, 1915.

Received for review January 29, 2001
Revised manuscript received May 14, 2001
Accepted May 15, 2001

IE0100941